Toxicol. Res.
Vol. 28, No. 1, pp. 39-49 (2012)
Open Access http://dx.doi.org/10.5487/TR.2012.28.1.039
pISSN: 1976-8257 eISSN: 2234-2753

Official Journal of Korean Society of Toxicology
Available online at http://www.toxmut.or.kr

Suppressive Effect of Zinc on the Formation of Colonic Preneoplastic Lesions in the Mouse Fed High Levels of Dietary Iron

Hyunji Park[1], Bong Su Kang[1], Dang Young Kim[1], Ja Seon Yoon[1], Jae-Hwang Jeong[2], Sang Yoon Nam[1], Young Won Yun[1], Jong-Soo Kim[1] and Beom Jun Lee[1]

[1]College of Veterinary Medicine and Research Institute of Veterinary Medicine, Chungbuk National University, Cheongju 361-763
[2]Department of Biotechnology and Biomedicine, Chungbuk Province College, Okcheon 373-807, Korea

(Received February 8, 2012; Revised March 18, 2012; Accepted March 28, 2012)

We investigated the effect of zinc on the formation of colonic aberrant crypt foci induced by azoxymethane (AOM) followed by dextran sodium sulfate (DSS) in mice with high iron diet (HFe; 450 ppm iron). Six-week old ICR mice were fed on high iron diets with combination of three different levels of zinc in diets, low-zinc (LZn; 0.01 ppm), medium-zinc (MZn; 0.1 ppm), and high-zinc (HZn; 1 ppm) for 12 weeks. Animals were received weekly intraperitoneal injections of AOM (10 mg/kg B.W. in saline) for 3 weeks followed by 2% DSS (molecular weight 36,000~50,000) in the drinking water for a week. To confirm the iron storage in the body, the hepatic iron concentration has been determine chemically and compared with histological assessment visualized by Prussian blue reaction. Aberrant crypt (AC) and aberrant crypt foci (ACF) were analyzed in the colonic mucosa of mouse fed high dietary iron. Superoxide dismutase (SOD) activity and thiobarbituric acid-reactive substances (TBARS) level were also investigated. Apoptosis in the preneoplastic lesion was determined by terminal deoxynucleotidyl transferase-mediated dUTP nickend labeling (TUNEL). In addition, immunohistochemistry of β-catenin was also performed on the mucous membrane of colon. The number of large ACF (≥ 4 AC/ACF), which possess greater tumorigenic potential, was significantly lower in MZn and HZn groups compared with LZn group. Cytosolic SOD activity in the liver was significantly higher in HZn group compared with LZn group. Hepatic MDA level was decreased significantly in HZn group compared with MZn and LZn groups. Apoptotic index was significantly higher in HZn group. Taken together, these findings indicate that dietary zinc might exert a protective effect against colonic preneoplastic lesion induced by AOM/DSS in ICR mice with high iron status, and suggest that dietary supplement of zinc might play a role in suppressing colon carcinogenesis in mice.

***Key words*:** Colon carcinogenesis, Zinc, Iron overload, Aberrant crypt foci (ACF), Mouse

INTRODUCTION

Colorectal cancer is one of the leading causes of cancer death in western countries or in the developed countries (Jemal *et al.*, 2011; Tanaka *et al.*, 2003). In Korea, the incidence and mortality of colorectal cancer have gradually increased in the last decade, becoming the fourth leading cause of cancer deaths (Korea National Statistical Office, 2011).

There are several chemical-induced experimental models of colon cancer in animal. The most commonly used colon carcinogens are 1,2-dimethylhydrazine (DMH) and its metabolite azoxymethane (AOM). The DMH or AOM-induced colon cancer shares many similarities to human sporadic colon cancer, including the response to some promotional and preventive agents (Corpet and Pierre, 2005). The ultimate carcinogenic metabolite of DMH causes methylation of the DNA bases of various organs, including epithelial cells of colonic crypts (Perse and Cerar, 2011). Thus, this results in a loss of colonic cells by apoptosis, an increase in proliferation and mutation of colonic epithelial cells (Chang, 1984). Dextran sodium sulfate (DSS) induces colonic inflammation in rodents and promotes colon carcinogenesis, thereby being used for experimental animal colorectal cancer model (Rosenberg *et al.*, 2009). AOM treatment during or after DSS administration do not generate a significant number of colonic neoplasm in mice, while DSS administration after

Correspondence to: Beom Jun Lee, Department of Veterinary Public Health, College of Veterinary Medicine, Chungbuk National University, Cheongju 361-763, Korea
E-mail: beomjun@cbu.ac.kr
or Jong-Soo Kim, Research Institute of Veterinary Medicine, Chungbuk National University, Cheongju 361-763, Korea
E-mail: jsvet@cbu.ac.kr

AOM treatment could induce a number of colonic neoplasm (Tanaka *et al.*, 2003).

By reason of relatively long developmental process of tumors, preneoplastic lesions can be used as biomarkers for assessing the risk of developing colon cancer or for identifying modulators of colon carcinogenesis in short-term studies (Bird, 1998). Aberrant crypt foci (ACF) were first reported on a method for directly visualizing altered crypts induced by carcinogens in the intact colon (Bird, 1987). ACF are the first lesion in the development of colon cancer that can be identified microscopically on methylene blue-stained colon mucosa. ACF are characterized by enlarged and elevated dark crypts and increases pericryptal space (Bird, 1987).

β-Catenin, acting as a structural protein and transcriptional activator-mediating Wnt signaling, is mostly localized at membranes of cell-to-cell border (Ross, 1981). β-catenin mutations were frequently observed in AOM-induced colon cancer in rodents (Hata *et al.*, 2004; Hirose *et al.*, 2003; Takahashi *et al.*, 1998). When β-catenin mutations occur, the protein localize to the cytoplasm or nucleus (Kobayashi *et al.*, 2000). Crypts with increased β-catenin expression have been suggested as a more relevant biomarker of colon cancer than ACF (Mori *et al.*, 2004; Yamada *et al.*, 2000).

Iron and zinc are micronutrients that were associated with many diseases including cancers. Many studies reported that iron may induce mutagenic effects mediated through free-radical generation or tumor promotion through nutritional mechanisms (Hann *et al.*, 1988; Stevens and Kalkwarf, 1990). As a transition metal, iron is capable of generating free radicals participating in lipid peroxidation reactions. Such reactions are thought to lead to DNA damage and, in some cases, neoplasia (Wurzelmann *et al.*, 1996). The iron that generates free radical via Fenton reaction is free iron, not iron bound to ferritin or transferrin. If antioxidants exist, the possible prooxidant effect of iron is countered (Lee *et al.*, 2004).

Zinc is vital for the function of all living systems. It is an essential trace element important for the stabilization and function of numerous metalloenzymes, especially copper-zinc superoxide dismutases (Sky-Peck, 1986). Zinc plays an important role in the metabolism and interaction of malignant cells (Evans and Halliwell, 2001; Schrauzer, 1977). Zinc has a stabilizing effect on membranes possibly by displacing bound transition metal ions and thereby preventing peroxidation of membrane lipids (Bettger *et al.*, 1980). Moreover, it was founded that zinc had a protective effect against colonic preneoplastic development induced by DMH in rats (Dani *et al.*, 2007).

Oxidative stress caused by reactive oxygen metabolites results in damage to cellular structure, thereby implicates in the initiation and promotion phases of carcinogenesis (Davis and Feng, 1999). Malondialdehyde (MDA), product of lipid peroxidation, is one of the most frequently used indicators of lipid peroxidation. MDA is a mutagenic and genotoxic agent that may contribute to the development of human cancer because of its high cytotoxicity and inhibitory action on protective enzymes (Feron *et al.*, 1991).

The aim of this study was to examine the role of dietary zinc in the formation of colonic preneoplastic lesions induced by AOM/ DSS in mice fed high dietary iron.

MATERIALS AND METHODS

Materials. Azoxymethane, potassium ferrocyanide, nuclear fast red, and aluminum sulfate were purchase from Sigma Chemical Company (St. Louis, MO, USA). Dextran sodium sulfate (molecular weight 36,000~50,000) was purchased from MP Biomedicals (Solon, OH, USA).

Animals. Male ICR mice aged 5 weeks were purchased from SLC Inc. (Shizuoka, Japan), and housed in polycarbonate cages (5 mice/cage). Animals were fed on customized diet based on AIN-93G controlled purified rodent diet (Dyets, Inc., Bethlehem, PA, USA) and water was provided *ad libitum*, under controlled condition of temperature (20 ± 2°C), relative humidity (50 ± 20%) and light (12/12 h light/dark cycle). The animal experiment was conducted in accordance with "Guide for care and use of laboratory animals" of Chungbuk National University. After one week of acclimatization, the animals were fed diets containing modified levels of iron and zinc. During the experimental period, weekly body weights and feed consumptions were recorded.

Experimental design. Twenty mice were assigned to each AOM/DSS treatment groups, while ten mice to vehi-

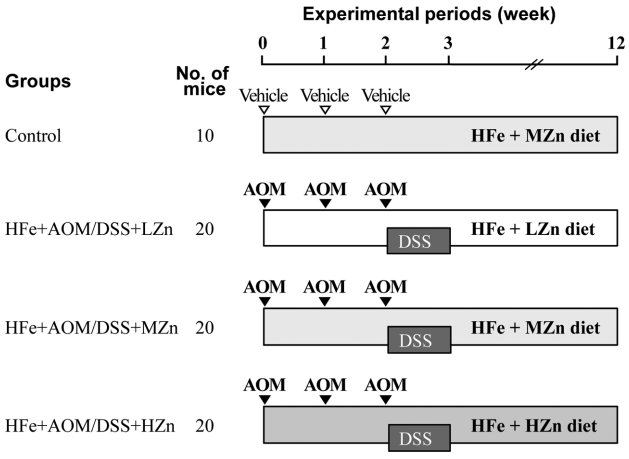

Fig. 1. Experimental design for colon carcinogenesis in mice fed high iron diet. AOM: Azoxymethane (10 mg/kg body weight in saline, intraperitoneal injection, weekly 3 times). DSS : Dextran sodium sulfate (2% drinking water for a week).

Table 1. Composition of the animal diets with high level of iron and different levels of zinc

Groups	HFe + LZn	HFe + MZn	HFe + HZn
Ingredients	g/kg	g/kg	g/kg
Casein	200	200	200
L-Cystine	3	3	3
Sucrose	54.7	52.9	34.9
Cornstarch	397.486	397.486	397.486
Dyetrose	132	132	132
Soybean Oil	70	70	70
t-Butylhydroquinone	0.014	0.014	0.014
Microcrystalline Cellulose	50	50	50
Mineral Mix #215020	35.1	35.1	35.1
Ferric Citrate (ppm as Fe)	450	450	450
Zinc Carbonate (ppm as Zn)	1	10	100
Vitamin Mix # 310025	10	10	10
Choline Bitartrate	2.5	2.5	2.5
Total gram	1000	1000	1000

cle control group (Fig. 1). For AOM/DSS treatment groups, animals were given a weekly intraperitoneal injection of AOM (10 mg/kg body weight in saline) for 3 weeks. After the last AOM injection, additional 2% DSS was given in the drinking water for 7 days. In the control group, mice were injected with saline instead of AOM and no additional DSS was given. The mice in the control group were fed the high iron (HFe; 450 ppm Fe) with medium-zinc diet (HFe + MZn; 10 ppm Zn). Additionally, the mice in three AOM/DSS treatment groups were fed a high iron with a low-zinc diet (HFe + LZn; 1 ppm Zn), a medium-zinc diet (HFe + MZn; 10 ppm Zn) and a high-zinc diet (HFe + HZn; 100 ppm Zn).

Animal diets. The AIN-93G purified rodent diet contained 20% casein, 0.3% L-cystine, 39.7% cornstarch, 13.2% dyetrose, 7% soybean oil, 0.0014% t-butylhydroquinone, 5% cellulose, 3.7% mineral mix, 1% vitamin mix, 0.25% choline bitartrate. The high iron diet contained ferric citrate at the level of 450 ppm as iron. Low-zinc diet (LZn), medium-zinc diet (MZn) and high-zinc diet (HZn) contained zinc carbonate at the level of 1, 10 and 100 ppm as zinc (Table 1).

Sample collection and blood analysis. Mice were sacrificed at 12 weeks after the experiment. After laparotomy, blood was collected by a syringe from the abdominal aorta and immediately transferred into tubes containing K_3-EDTA and serum separator tubes (Vacutainer, Becton Drive Franklin Lakes, NJ, USA). The liver and entire large intestine were harvested. One fifth of liver tissue was washed with saline, blot dried, weighed and then frozen in liquid nitrogen. A half of the large intestine from cecum to anus was longitudinally opened, flushed with saline, and fixed in 10% neutral buffered formalin. The other half was washed with saline, blot dried and then frozen in liquid nitrogen. Blood samples in EDTA tubes were used for analysis of complete blood cell count with Abbott CellDyn-3500 (Abbott Laboratories, Chicago, IL, USA).

Analysis of hepatic iron. For the determination of total iron concentrations in the liver, frozen liver tissues were digested and ashed at 200°C for 4 h using concentrated nitric acid and hydrogen peroxide, and analysed by inductively coupled plasma spectrophotometer (ICP-AES, JY 38 Plus, JOBIN-YVON, France).

Hepatic SOD activity assay. Superoxide dismutase (SOD) activity was measured using a commercial assay kit (Cayman, MI, USA) according to manufacturer's instructions. This kit utilizes a tetrazolium salt for the detection of superoxide radicals generated by xanthine oxidase and hypoxanthine. One unit of SOD was defined as the amount of enzyme needed to produce 50% dismutation of superoxide radicals. To separate SOD, liver homogenate was centrifuged at 1500 ×g for 10 min and the supernatant was centrifuged at 10,000 ×g for 15 min at 4°C. The resulting 10,000 ×g supernatant, containing cytosolic SOD, was collected and analyzed for SOD activity.

Determination of lipid peroxidation in liver. The level of malondialdehyde (MDA), an end product of lipid peroxidation, was determined in the liver. The amounts of MDA contained in the tissue homogenate were measured using a thiobarbituric acid reactive substance (TBARS) assay kit (Cayman, MI, USA) according to manufacturer's instructions. In brief, MDA-TBA adduct was formed by the reaction of MDA and TBA under high temperature (90~100°C) and acidic condition. The MDA-TBA adduct appeared as pink chromogen, and was measured at 532 nm.

Analysis of aberrant crypt (AC) and aberrant crypt foci (ACF). The colon was removed and washed thoroughly with 0.85% NaCl solution and fixed with 10% neutral buffered formalin. The colon was then stained with 0.5% methylene blue solution for 30 sec in order to identify AC and ACF. The numbers of ACF and AC in each focus were counted under a microscope. ACF were identified with the following morphological characteristics: 1) the enlarged and elevated crypts than normal mucosa, and 2) increased pericryptal space and irregular lumens (McLellan and Bird, 1988).

Histopathological examination. The colon tissues fixed in 10% neutral buffered formalin were paraffin-embedded, cut to multiple 4-μm sections, and stained with hematoxylin and eosin for histopathological examination. For the identification of ferric ion in the liver, paraffin-embedded tissue sections were deparaffinized, rehydrated, and incubated in a ferrocyanide solution (20% hydrochloric acid and 10% potassium ferrocyanide) at 60°C for 20 min. Nuclear fast red (0.1% in 5% aluminum sulfate solution) was used for a counter-stain.

Immunohistochemistry. Immunohistochemistry for proliferating cell nuclear antigen (PCNA) and β-catenin was performed on 4-μm formalin-fixed, paraffin-embedded distal colon sections. The sections were subjected to deparaffinization and hydration prior to quenching of endogenous peroxidase activity (3% H_2O_2 in methanol for 15 min). The sections were incubated for 60 min with the primary anti-PCNA mouse monoclonal antibody and anti-β-catenin rabbit polyclonal antibody (Santa Cruz Biotechnology, Santa Cruz, CA, USA). Slides were processed with the ABC reagent from Vectastain Elite kit (Vector Laboratories, Burlingame, CA, USA) and developed with the 3,3′-diaminobenzidine, tetrahydrochloride (DAB) chromogen. The sections were counter-stained with mayer hematoxylin. Twenty fields, randomly selected from each slide, were analyzed at 100× magnification. The numbers of nuclei with positive reactivity for PCNA immunohistochemistry were counted in a total of 3 × 100 cells in 3 different areas of the colonic cancer (Tanaka *et al.*, 2010). The expression of β-catenin was graded by intensity of nuclear staining accompanied by loss of membranous staining as negative (localization limited to membrane), focal positive (positive cells clustered in focal area) and diffuse positive (positive cells distributed diffusely), described by Kobayashi *et al*. (2000). Cytoplasmic immunoreactivity was not considered in this study because the expression was variable and not clearly related to the shift from membranous to nuclear staining.

TUNEL assay. Levels of apoptosis in distal colon tissue were determined using the TdT-mediated dUTP nick-end labeling (TUNEL) method. The 4-μm formalin-fixed, paraffin-embedded tissue sections from the distal colon were processed according to manufacturer's instructions for the ApopTag peroxidase *in situ* apoptosis detection kit (TUNEL; Vector Laboratories, Burlingame, CA, USA). The numbers of nuclei with positive reactivity for TUNEL assay were counted in a total of 3 × 100 cells in 3 different areas of the colonic mucosa (Tanaka *et al*., 2010).

Statistical analysis. Data of ACF, PCNA and TUNEL assay were analyzed by Dunn's multiple comparison test after Kruskal-Wallis' nonparametric analysis of variance. Difference in nuclear expression pattern of β-catenin in the colon among the AOM/DSS treated groups was analyzed by chi-square independent test. Other parametric data were analyzed by one-way analysis of variance and significant differences among treatment groups were evaluated by Tukey-Kramer test. For all comparisons, $p < 0.05$ was considered statistically significant.

RESULTS

Changes in body weights and hematology. There were no significant differences in body weight among the AOM/DSS treated experimental groups. All of the AOM/DSS-treated groups showed significant decreases in body weights at the end of experiment compared with vehicle control group ($p < 0.05$) (Table 2). The lowered body weights of mice in AOM/DSS-treated groups seemed to be related to the reduction of feed consumption.

There were no significant differences among the groups in red blood cell counts, white blood cell counts, hemoglobin, hematocrit, mean corpuscular volume, mean corpuscular hemoglobin, and mean corpuscular hemoglobin concentration. Thus, high iron diets did not induce changes in hematologic values regardless of AOM/DSS treatment. Low-zinc diet group showed slightly lower white blood cell counts but it was not statistically significant (Table 2).

Total number of aberrant crypt (AC) and aberrant crypt foci (ACF). The animals in vehicle control group showed no evidence of AC or ACF formation in the colon with high iron diet. The number of AC in high-zinc diet group (18.00 ± 0.79) was significantly lower than low-zinc diet group (26.14 ±1.01) ($p < 0.05$). The number of ACF in high-zinc diet group (6.53 ± 0.37) was significantly lower than in low-zinc diet group (8.38 ± 0.53) and medium-zinc diet group (8.40 ± 0.43) ($p < 0.05$) (Fig. 2).

Number of aberrant crypt foci (ACF). There was no significant change in the number of small ACF (≤ 3 AC/ACF) among experimental groups. However, the number of large ACF (≥ 4 AC/ACF) in MZn group (1.47 ± 0.19 ACF/colon) and in HZn group (1.00 ± 0.08 ACF/colon) were significantly lower than LZn group (2.43 ± 0.21 ACF/colon)

Table 2. Final body weights and hematology in mice fed high iron diet

		Control	AOM/DSS		
			LZn	MZn	HZn
Final body weights (g)		42.25 ± 0.63[a]	39.36 ± 0.42[b]	39.87 ± 0.60[b]	38.56 ± 0.27[b]
Hematology	WBC (thousands)	1.74 ± 0.15	1.00 ± 0.08	2.19 ± 0.29	1.74 ± 0.54
	RBC (millions)	8.79 ± 0.21	7.93 ± 0.39	7.61 ± 0.71	7.29 ± 1.29
	Hb (g/dl)	13.40 ± 0.33	12.65 ± 0.60	11.80 ± 1.64	11.73 ± 1.57
	HCT (%)	45.60 ± 1.32	41.55 ± 1.90	40.00 ± 4.11	39.37 ± 5.00
	MCV (fl)	51.90 ± 0.99	52.45 ± 0.69	52.40 ± 1.36	55.30 ± 3.78
	MCH (pg)	15.23 ± 0.27	16.00 ± 0.27	15.30 ± 1.00	16.37 ± 0.95
	MCHC (g/dl)	29.38 ± 0.11	30.50 ± 0.22	29.10 ± 1.34	29.70 ± 0.31

AOM: azoxymethane, DSS: dextran sodium sulfate LZn: low-zinc diet, MZn: medium-zinc diet, HZn: high-zinc diet, WBC: white blood cells, RBC: red blood cells, Hb: hemoglobin, HCT: hematocrit, MCV: mean corpuscular volume, MCH: mean corpuscular hemoglobin, MCHC: mean corpuscular hemoglobin concentration, Data represented as mean ± SEM.
[ab]Means with different letter were significantly different ($p < 0.05$).

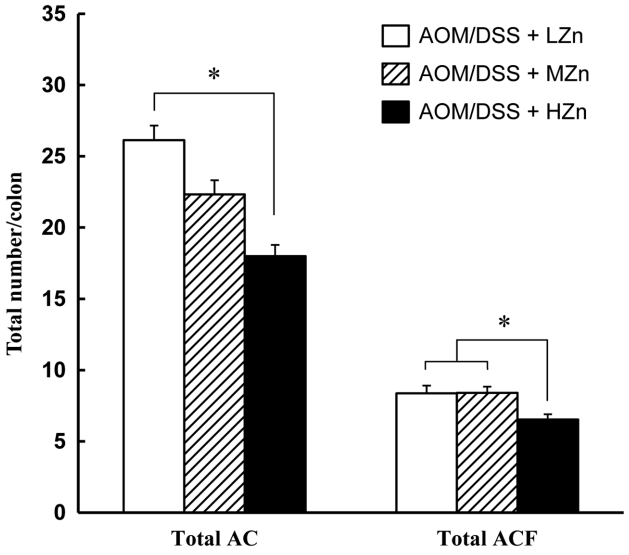

Fig. 2. Effect of zinc on colonic aberrant crypt and aberrant crypt foci formation in mice fed high iron diet. Control group showed no evidence of AC or ACF formation in the colon with high iron diet. The number of AC in HZn group was significantly lower than LZn group (*$p < 0.05$). The number of ACF in HZn group was significantly lower than in LZn group and in MZn group, respectively (*$p < 0.05$). Values are mean ± SEM. AC: aberrant crypt, ACF: aberrant crypt foci, AOM: azoxymethane, DSS: dextran sodium sulfate, LZn: low-zinc diet, MZn: medium-zinc diet, HZn: high-zinc diet.

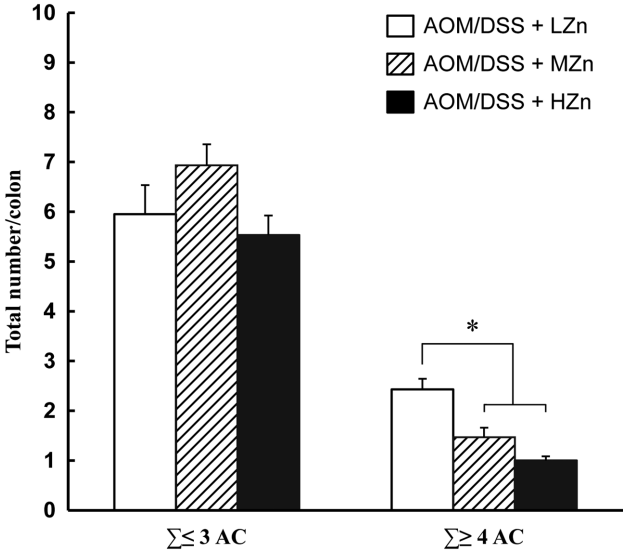

Fig. 3. Effect of zinc on colonic aberrant crypt formation in mice fed high iron diet. The numbers of large ACF (≥ 4 AC/ACF), which possess greater tumorigenic potential, in MZn group and in HZn group were significantly lower compared with LZn group (*$p < 0.05$). Values are mean ± SEM. AC: aberrant crypt, ACF: aberrant crypt foci, AOM: azoxymethane, DSS: dextran sodium sulfate, LZn: low-zinc diet, MZn: medium-zinc diet, HZn: high-zinc diet.

($p < 0.05$) (Fig. 3).

Hepatic iron level. In order to confirm Fe-load in the body by dietary supplement of iron, the iron concentrations in the liver were analyzed by ICP-AES. AOM/DSS treatment did not induce the changes in hepatic iron concentration. Regardless of dietary zinc concentration, the levels of hepatic iron concentration were similar among the groups (Fig. 4). Numerous Prussian blue reactive iron deposits were detected in the liver of mice fed high iron diet (Fig. 5).

SOD in the liver. The levels of SOD in LZn group (10.01 ± 1.01) and MZn group (13.21 ± 0.29) were not significantly different from that in the control group (9.51 ± 0.91). In AOM/DSS treated groups, the levels of SOD were increased in a dose-dependent manner with increasing zinc levels in diets. HZn group (18.12 ± 1.53) showed significantly higher SOD level compared with LZn group ($p <$

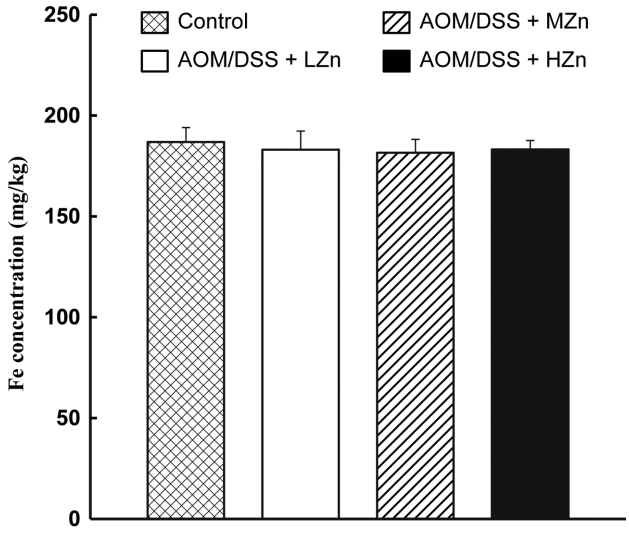

Fig. 4. Hepatic iron levels in mice fed high iron diet. AOM/DSS treatment did not induce the changes in hepatic iron concentration. Regardless of dietary zinc concentration, the levels of hepatic iron concentration were similar among the groups. Values are mean ± SEM. AOM: azoxymethane, DSS: dextran sodium sulfate, LZn: low-zinc diet, MZn: medium-zinc diet, HZn: high-zinc diet.

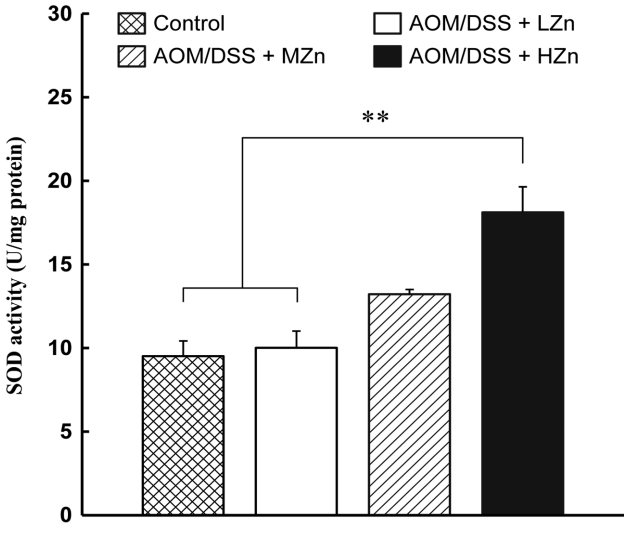

Fig. 6. Effect of zinc on superoxide dismutase (SOD) in the liver of mice fed high iron diet. In AOM/DSS treated groups, the levels of SOD were increased in a dose-dependent manner with increasing zinc levels in diets. HZn group shows significantly higher SOD level compared with LZn group (**$p < 0.01$). Values are mean ± SEM. AOM: azoxymethane, DSS: dextran sodium sulfate, LZn: low-zinc diet, MZn: medium-zinc diet, HZn: high-zinc diet.

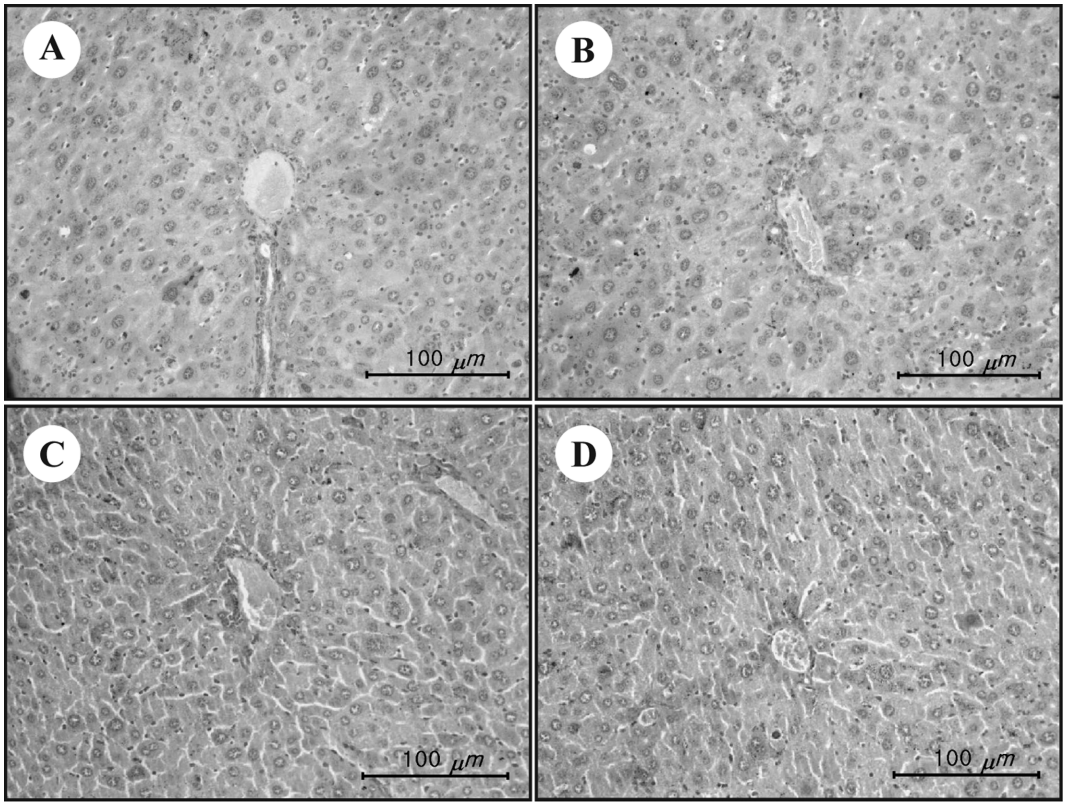

Fig. 5. Perls' Prussian blue staining for the detection of hepatic iron in mice fed high iron diet. Numerous Prussian blue reactive iron deposits are seen in the liver of mice fed high iron diet. (A) Control group, (B) AOM/DSS + low-zinc diet group, (C) AOM/DSS + medium-zinc diet group, (D) AOM/DSS + high-zinc diet group.

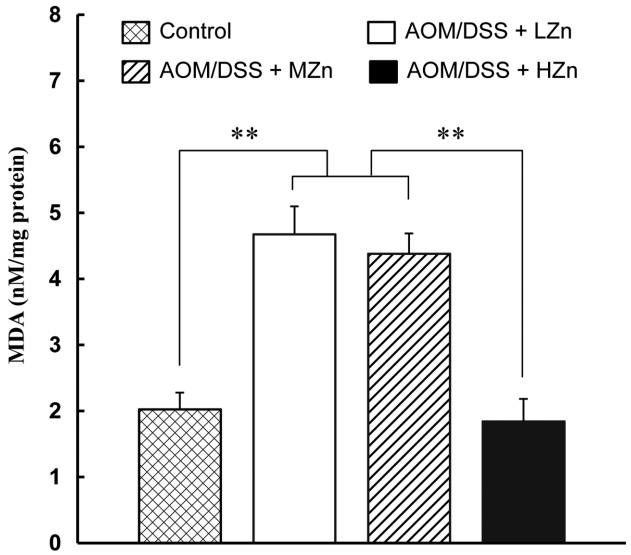

Fig. 7. Effect of zinc on lipid peroxidation in the liver of mice fed high iron diet. Lipid peroxidation in the liver of HZn group was significantly decreased compared with MZn and LZn group in iron-overloaded status (**$p < 0.01$). Values are mean ± SEM. AOM: azoxymethane, DSS: dextran sodium sulfate, LZn: low-zinc diet, MZn: medium-zinc diet, HZn: high-zinc diet.

0.01) (Fig. 6).

MDA in the liver. LZn group (4.68 ± 0.42) showed the highest level of MDA among AOM/DSS treated experimental groups in the liver. In HZn group (1.84 ± 0.35) the level of MDA was significantly lower than that of LZn group (4.68 ± 0.42) or MZn group (4.38 ± 0.31), respectively ($p < 0.01$) (Fig. 7).

Histopathology. Vehicle control group displayed normal colonic architecture with no sign of apparent abnormality. In AOM/DSS-treated groups, thickened epithelium and both dysplasia and/or hyperplasia were observed (Fig. 8).

Changes in cell proliferation and apoptosis in colon. Cell proliferation was evaluated by quantification of PCNA-positive cells. The PCNA-positive cells were significantly increased in the AOM/DSS treated groups, while few PCNA-positive cells were observed at the bottom of crypts in control group. The number of PCNA-positive cells was the highest in the mice fed low-zinc diet, but there were no significant differences in proliferative indices among the AOM/DSS treated experimental groups (Fig. 9).

Apoptotic bodies were visualized by TUNEL method.

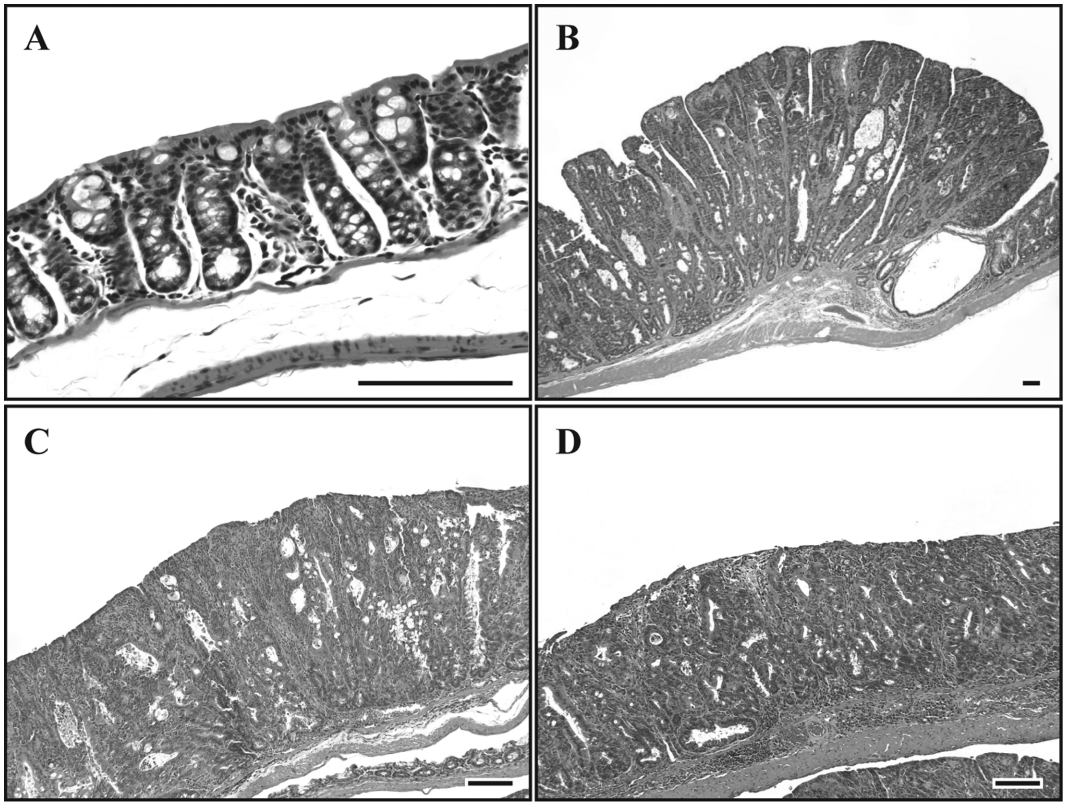

Fig. 8. Histopathology of colonic epithelium of mice fed high iron diet. Control group shows normal colonic architecture with no sign of abnormality. Thickened epithelium and hyperplasia are seen in AOM/DSS-treated groups. (A) Control group, (B) AOM/DSS + low-zinc diet group, (C) AOM/DSS + medium-zinc diet group, (D) AOM/DSS + high-zinc diet group. Bar = 10 μm.

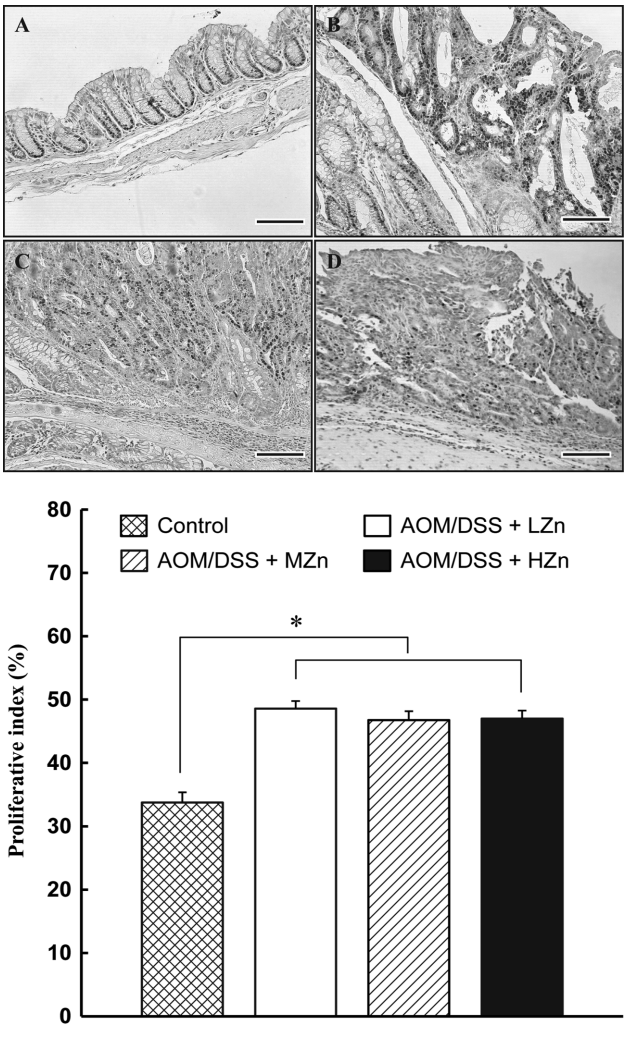

Fig. 9. Immunohistochemistry of PCNA and proliferative index in the colon of mice fed high iron diet. Treatments of AOM/DSS induced the increases in PCNA-positive cells, while few PCNA-positive cells are seen at the bottom of crypts in control group. (A) Control group, (B) AOM/DSS + low-zinc diet group, (C) AOM/DSS + medium-zinc diet group, (D) AOM/DSS + high-zinc diet group. Bar = 10 μm. There were no significant differences in proliferative indices among the AOM/DSS treated experimental groups. Values are mean ± SEM. *Significantly different ($p < 0.05$).

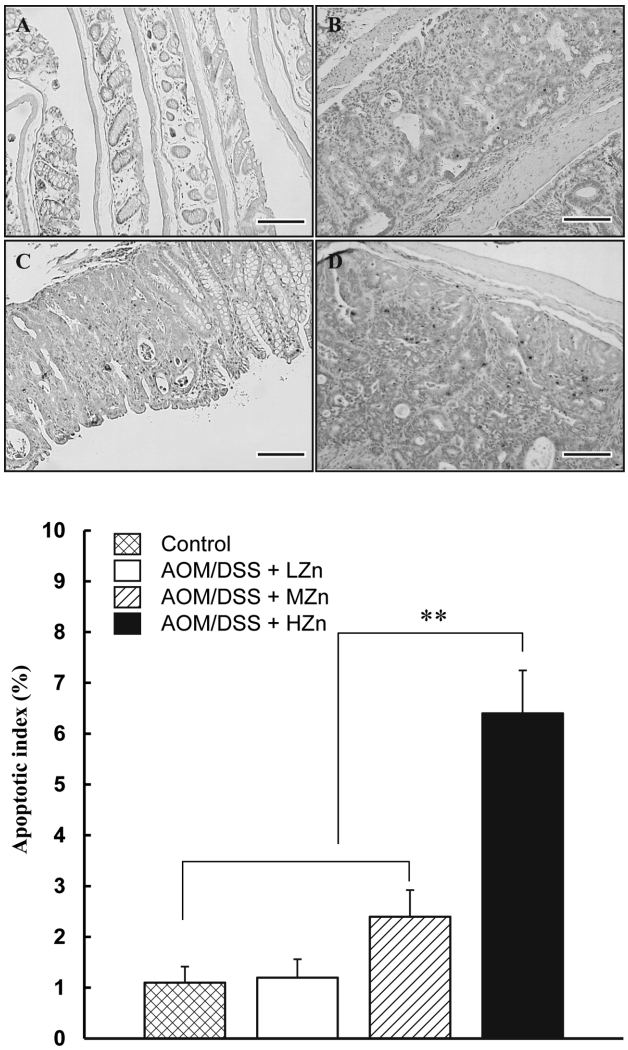

Fig. 10. TUNEL assay for apoptotic nuclei and apoptotic index in the distal colon of mice fed high iron diet. Apoptotic bodies were visualized by TUNEL method. (A) Control group, (B) AOM/DSS + low-zinc diet group, (C) AOM/DSS + medium-zinc diet group, (D) AOM/DSS + high-zinc diet group. Bar = 10 μm. A significant increase in TUNEL-positive cells were observed in high-zinc diet group (**$p < 0.01$). Values are mean ± SEM.

The colon epithelium of the mice in HZn group represented a markedly higher count of apoptotic bodies compared with control and other AOM/DSS-treated groups ($p < 0.01$) (Fig. 10).

Immunohistochemistry of β-catenin. A variation of the nuclear staining was detected in the epithelial cells of colonic mucosa. The colonic mucosa of control group did not show the nuclear localization of β-catenin (Fig. 11A). Strong cytoplasmic and nuclear β-catenin immunoreactivities were observed on the epithelial cells of LZn and MZn groups (Fig. 11B, C). On the other hand, the nuclear β-catenin immunoreactivity in HZn group was weak (Fig. 11D). No significant differences were found in the number of cells with nuclear β-catenin expression among the AOM/DSS treated groups, and in the distribution of β-catenin expression patterns (data not shown).

DISCUSSION

Colon is the most common site for malignancies of gastrointestinal tract and colorectal cancer is the second leading cause of cancer death in male of developed countries (Jemal *et al.*, 2011). Moreover, colon cancer does not

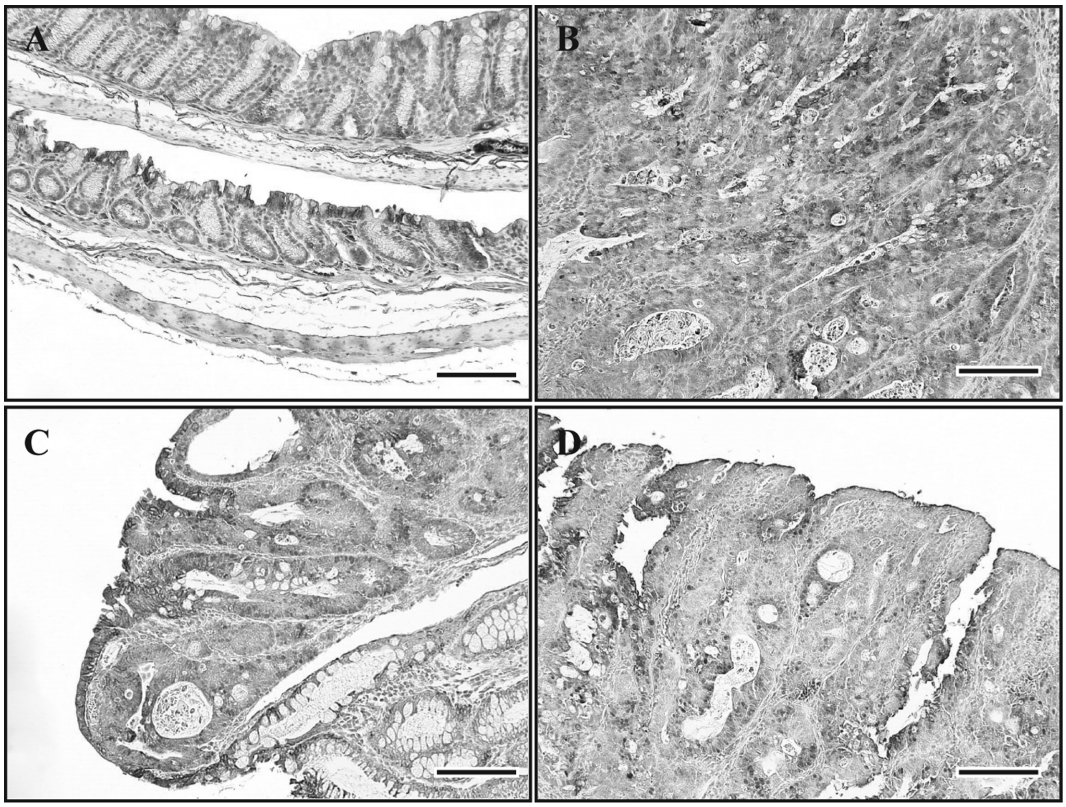

Fig. 11. Immunohistochemistry of β-catenin on distal colon of mice fed high iron diet. The colonic mucosa of control group did not show the nuclear localization of β-catenin (A). Strong cytoplasmic and nuclear β-catenin immunoreactivities were observed on the epithelial cells of low-zinc diet group (B) and medium-zinc diet group (C). The nuclear β-catenin immunoreactivity in high-zinc diet group (D) was weak. Bar = 10 μm.

appear to be a result of aging, but is intrinsically associated with dietary pattern. Red and processed meat consumption promotes the risk of colorectal cancer, and this promotion is found to correlate closely with dietary iron (Doll and Peto, 1981). Dani *et al*. (2007) reported that zinc inhibited the formation of ACF suggesting the potential of zinc in suppressing the progression of preneoplasia to malignant neoplasia and the suppressing effect of zinc could be explained by its putative antioxidant activity.

High dietary intakes of iron may induce an abnormal iron accumulation, an increased lipid peroxidation and the risk of colon cancer, due to the ability of iron to generate free radicals *in vivo* (Evans and Halliwell, 2001).

In this study, we examined the effects of zinc on the formation of colonic preneoplastic lesions induced by AOM/DSS with high level of dietary iron in mice. High iron diet did not induce changes in hematologic values regardless of AOM/DSS treatment. Biochemical and histological analysis showed that high dietary iron induce uniform accumulation of iron in the liver regardless of AOM/DSS treatment or changes in dietary zinc level.

ACF are putative preneoplastic lesions that have been detected in human colon cancer and experimental animals treated with chemical carcinogen. ACF can be identified microscopically on the surface of the whole mount colon mucosa after methylene blue staining. They are distinguished from normal crypts by their larger size, darker staining and increased pericryptal space (Bird, 1987).

In this study, total number of AC and ACF were significantly lower in HZn group compared with LZn group. In addition, the number of large ACF (≥ 4 AC/ACF), which possess greater tumorigenic potential (McLellan *et al.*, 1991), was significantly decreased in MZn group and in HZn group compared with LZn group. These results suggest that dietary supplement of zinc induces an inhibition of AC and ACF formation in iron overloaded status.

Colon carcinogenesis is a pathological consequence of persistent oxidative stress, leading to DNA damage and multiple genetic changes that may be caused by overproduction of reactive oxygen species in cancer-related genes (Bartsch and Nair, 2002).

The enzyme SOD promotes the conversion of superoxide free-radical anions into hydrogen peroxide. SOD has been shown to have a protective effect against lipid peroxidation (Sun *et al.*, 2005). The levels of SOD in LZn and MZn group were not significantly different from control group.

However, the level of SOD in HZn group was significantly higher compared with LZn group. These findings suggest that high zinc diet play an effective role in promotion of SOD activity in iron-overloaded status.

Oxidative stress can result in cellular injury due to lipid peroxidation, DNA damage and mutagenesis, and it has been associated with various stage of tumor formation process (Halliwell and Gutteridge, 1989; Stohs and Bagchi, 1995). Thiobarbituric acid reacts with MDA or MDA-like derives formed during the oxidative decomposition of polyunsaturated fats to form a colored product (Rael *et al.*, 2004). Lipid peroxidation in the liver of HZn group was significantly decreased compared with MZn and LZn group in iron-overloaded status. These findings suggest that dietary zinc may play a protective role in colonic carcinogenesis through the regulation of lipid peroxidation.

PCNA is a non-histone nuclear protein and associated with DNA synthesis phase of the cell cycle, and frequently used for the marker of cell proliferation. Dietary zinc did not induce any changes in cell proliferation induced by AOM/DSS in colonic epithelial cells in this study.

TUNEL assay is a method for detecting DNA fragmentation by labeling the terminal end of nucleic acids (Grasl-Kraupp *et al.*, 1995). TUNEL of normal rodent large intestine stains only the uppermost nuclei at the edge of the crypt facing the lumen, while the rest of the crypt remains unstained (Gavrieli *et al.*, 1992). TUNEL assay was performed in order to confirm the association between dietary zinc levels and apoptosis of tumorigenic cells induced by AOM/DSS in iron-overloaded status. The epithelium of colon in HZn group represented a markedly higher count of apoptotic bodies compared with other AOM/DSS-treated groups (LZn and MZn), indicating that high dietary zinc might induce upregulation of programmed cell death of tumorigenic cells.

β-Catenin is an important factor in Wnt signaling and thereby regulating transcription of genes related to proliferation and development of cells (Miller and Moon, 1996). In colon carcinogenesis, β-catenin accumulates in nucleus and/or cytosol. Alteration of β-catenin may play an important role in causing early dysplastic change (Takahashi *et al.*, 1998). β-Catenin expression was mostly localized at membranes of colonic mucosa in control group. LZn and MZn groups showed an increased nuclear β-catenin expression compared with HZn group. Especially in LZn group, strong β-catenin expression was seen in the nucleus and cytoplasm. However, more detailed quantitative analysis is required to conclude the relationship between dietary zinc level and β-catenin mutation.

In conclusion, in the status of iron-overload, high dietary zinc reduced the formation of colonic preneoplastic lesion (AC, ACF) and multiplicity of ACF, promoted hepatic SOD activity, reduced lipid peroxidation, and upregulated apoptosis of tumorigenic cells induced by AOM/DSS. These findings suggest that zinc may play a possible protective role in colon carcinogenesis in mice.

ACKNOWLEDGEMENTS

This work was supported by Priority Research Centers Program through the National Research Foundation of Korea (NRF) funded by the Ministry of Education, Science and Technology (2011-0031403) and National Research Foundation Grant funded by the Ministry of Education, Science and Technology (NRF-2008-313-E00628).

REFERENCES

Bartsch, H. and Nair, J. (2002). Potential role of lipid peroxidation derived DNA damage in human colon carcinogenesis: studies on exocyclic base adducts as stable oxidative stress markers. *Cancer Detect. Prev.*, **26**, 308-312.

Bettger, W.J., Reeves, P.G., Savage, J.E. and O'Dell, B.L. (1980). Interaction of zinc and vitamin E in the chick. *Proc. Soc. Exp. Biol. Med.*, **163**, 432-436.

Bird, R.P. (1998). Aberrant crypt foci system to study cancer preventive agents in the colon. In *Tumor Marker Protocols*. (M. Hanausek and Z. Walaszek Eds.). Humana Press, Totowa, pp. 465-474.

Bird, R.P. (1987). Observation and quantification of aberrant crypts in the murine colon treated with a colon carcinogen: preliminary findings. *Cancer Lett.*, **37**, 147-151.

Chang, W.W. (1984). Histogenesis of colon cancer in experimental animals. *Scand. J. Gastroenterol. Suppl.*, **104**, 27-43.

Corpet, D.E. and Pierre, F. (2005). How good are rodent models of carcinogenesis in predicting efficacy in humans? A systematic review and meta-analysis of colon chemoprevention in rats, mice and men. *Eur. J. Cancer*, **41**, 1911-1922.

Dani, V., Goel, A., Vaiphei, K. and Dhawan, D.K. (2007). Chemopreventive potential of zinc in experimentally induced colon carcinogenesis. *Toxicol. Lett.*, **171**, 10-18.

Davis, C.D. and Feng, Y. (1999). Dietary copper, manganese and iron affect the formation of aberrant crypts in colon of rats administered 3,2′-dimethyl-4-aminobiphenyl. *J. Nutr.*, **129**, 1060-1067.

Doll, R. and Peto, R. (1981). The causes of cancer: quantitative estimates of avoidable risks of cancer in the United States today. *J. Natl. Cancer Inst.*, **66**, 1191-1308.

Evans, P. and Halliwell, B. (2001). Micronutrients: oxidant/antioxidant status. *Br. J. Nutr.*, **85 Suppl 2**, S67-74.

Feron, V.J., Til, H.P., de Vrijer, F., Woutersen, R.A., Cassee, F.R. and van Bladeren, P.J. (1991). Aldehydes: occurrence, carcinogenic potential, mechanism of action and risk assessment. *Mutat. Res.*, **259**, 363-385.

Gavrieli, Y., Sherman, Y. and Ben-Sasson, S.A. (1992). Identification of programmed cell death in situ via specific labeling of nuclear DNA fragmentation. *J. Cell Biol.*, **119**, 493-501.

Grasl-Kraupp, B., Ruttkay-Nedecky, B., Koudelka, H., Bukowska, K., Bursch, W. and Schulte-Hermann, R. (1995). In situ detection of fragmented DNA (TUNEL assay) fails to discriminate among apoptosis, necrosis, and autolytic cell death: a cautionary note. *Hepatology*, **21**, 1465-1468.

Halliwell, B. and Gutteridge, J.M.C. (1989). Protection against oxidants in biological systems: The superoxide theory of oxygen toxicity. In *Free Radicals in Biology and Medicine*. (B. Halliwell and J.M.C. Gutteridge Eds.). Clarendon Press, Oxford, pp. 86-179.

Hann, H.W., Stahlhut, M.W. and Blumberg, B.S. (1988). Iron nutrition and tumor growth: decreased tumor growth in iron-deficient mice. *Cancer Res.*, **48**, 4168-4170.

Hata, K., Yamada, Y., Kuno, T., Hirose, Y., Hara, A., Qiang, S.H. and Mori, H. (2004). Tumor formation is correlated with expression of beta-catenin-accumulated crypts in azoxymethane-induced colon carcinogenesis in mice. *Cancer Sci.*, **95**, 316-320.

Hirose, Y., Kuno, T., Yamada, Y., Sakata, K., Katayama, M., Yoshida, K., Qiao, Z., Hata, K., Yoshimi, N. and Mori, H. (2003). Azoxymethane-induced beta-catenin-accumulated crypts in colonic mucosa of rodents as an intermediate biomarker for colon carcinogenesis. *Carcinogenesis*, **24**, 107-111.

Jemal, A., Bray, F., Center, M.M., Ferlay, J., Ward, E. and Forman, D. (2011). Global cancer statistics. *CA. Cancer J. Clin.*, **61**, 69-90.

Kobayashi, M., Honma, T., Matsuda, Y., Suzuki, Y., Narisawa, R., Ajioka, Y. and Asakura, H. (2000). Nuclear translocation of beta-catenin in colorectal cancer. *Br. J. Cancer*, **82**, 1689-1693.

Korea National Statistical Office (2011). Death and cause of death statistics 2010, KNSO, Daejeon.

Lee, D.H., Anderson, K.E., Harnack, L.J., Folsom, A.R. and Jacobs, D.R., Jr. (2004). Heme iron, zinc, alcohol consumption, and colon cancer: Iowa Women's Health Study. *J. Natl. Cancer Inst.*, **96**, 403-407.

McLellan, E.A. and Bird, R.P. (1988). Aberrant crypts: potential preneoplastic lesions in the murine colon. *Cancer Res.*, **48**, 6187-6192.

McLellan, E.A., Medline, A. and Bird, R.P. (1991). Dose response and proliferative characteristics of aberrant crypt foci: putative preneoplastic lesions in rat colon. *Carcinogenesis*, **12**, 2093-2098.

Miller, J.R. and Moon, R.T. (1996). Signal transduction through beta-catenin and specification of cell fate during embryogenesis. *Genes Dev.*, **10**, 2527-2539.

Mori, H., Yamada, Y., Kuno, T. and Hirose, Y. (2004). Aberrant crypt foci and beta-catenin accumulated crypts; significance and roles for colorectal carcinogenesis. *Mutat. Res.*, **566**, 191-208.

Perse, M. and Cerar, A. (2011). Morphological and molecular alterations in 1,2 dimethylhydrazine and azoxymethane induced colon carcinogenesis in rats. *J. Biomed. Biotechnol.*, **2011**, 473964.

Rael, L.T., Thomas, G.W., Craun, M.L., Curtis, C.G., Bar-Or, R. and Bar-Or, D. (2004). Lipid peroxidation and the thiobarbituric acid assay: standardization of the assay when using saturated and unsaturated fatty acids. *J. Biochem. Mol. Biol.*, **37**, 749-752.

Rosenberg, D.W., Giardina, C. and Tanaka, T. (2009). Mouse models for the study of colon carcinogenesis. *Carcinogenesis*, **30**, 183-196.

Ross, J.S. (1981). Experimental large intestinal adenocarcinoma induced by hydrazine and human colorectal cancer: a comparative study. In *Colonic Carcinogenesis*. (R.A. Malt and R.N. Williamson Eds.). MTP Press Limited, Lancaster, Boston, The Hague, pp. 187-207.

Schrauzer, G.N. (1977). Trace elements, nutrition and cancer: perspectives of prevention. *Adv. Exp. Med. Biol.*, **91**, 323-344.

Sky-Peck, H.H. (1986). Trace metals and neoplasia. *Clin. Physiol. Biochem.*, **4**, 99-111.

Stevens, R.G. and Kalkwarf, D.R. (1990). Iron, radiation, and cancer. *Environ. Health Perspect.*, **87**, 291-300.

Stohs, S.J. and Bagchi, D. (1995). Oxidative mechanisms in the toxicity of metal ions. *Free Radic. Biol. Med.*, **18**, 321-336.

Sun, J.Y., Jing, M.Y., Weng, X.Y., Fu, L.J., Xu, Z.R., Zi, N.T. and Wang, J.F. (2005). Effects of dietary zinc levels on the activities of enzymes, weights of organs, and the concentrations of zinc and copper in growing rats. *Biol. Trace Elem. Res.*, **107**, 153-165.

Takahashi, M., Fukuda, K., Sugimura, T. and Wakabayashi, K. (1998). Beta-catenin is frequently mutated and demonstrates altered cellular location in azoxymethane-induced rat colon tumors. *Cancer Res.*, **58**, 42-46.

Tanaka, T., de Azevedo, M.B., Duran, N., Alderete, J.B., Epifano, F., Genovese, S., Tanaka, M. and Curini, M. (2010). Colorectal cancer chemoprevention by 2 beta-cyclodextrin inclusion compounds of auraptene and 4′-geranyloxyferulic acid. *Int. J. Cancer*, **126**, 830-840.

Tanaka, T., Kohno, H., Suzuki, R., Yamada, Y., Sugie, S. and Mori, H. (2003). A novel inflammation-related mouse colon carcinogenesis model induced by azoxymethane and dextran sodium sulfate. *Cancer Sci.*, **94**, 965-973.

Wurzelmann, J.I., Silver, A., Schreinemachers, D.M., Sandler, R.S. and Everson, R.B. (1996). Iron intake and the risk of colorectal cancer. *Cancer Epidemiol. Biomarkers Prev.*, **5**, 503-507.

Yamada, Y., Yoshimi, N., Hirose, Y., Kawabata, K., Matsunaga, K., Shimizu, M., Hara, A. and Mori, H. (2000). Frequent beta-catenin gene mutations and accumulations of the protein in the putative preneoplastic lesions lacking macroscopic aberrant crypt foci appearance, in rat colon carcinogenesis. *Cancer Res.*, **60**, 3323-3327.